

4D RECONSTRUCTION FOR GATED CARDIAC SPECT USING FOURIER BASIS FUNCTIONS

Xiaofeng Niu and Yongyi Yang

Department of Electrical and Computer Engineering
Illinois Institute of Technology, Chicago, IL 60616, USA

ABSTRACT

A challenge in gated cardiac single photon emission computed tomography (SPECT) is the presence of increased imaging noise owing to gated data acquisition. In this study we propose a joint reconstruction approach for gated SPECT in which the different gate frames are reconstructed in a collective fashion by taking advantage of the statistics of the acquired data. Besides spatial smoothing, we use Fourier basis functions to regulate the time activities at each spatial location across the different gates, which are periodic owing to the periodic cardiac motion. We demonstrate the proposed approach by simulating gated Tc-99m labeled sestamibi imaging based on the NURBS-based cardiac-torso (NCAT) phantom.

Index Terms--- Gated SPECT, 4D reconstruction, spatio-temporal processing, Fourier basis functions

1. INTRODUCTION

Single photon emission computed tomography (SPECT) is one of the most prevalent diagnostic imaging techniques in use for diagnosis and evaluation of cardiac diseases. In gated cardiac SPECT, the data acquisition is synchronized to the electrocardiogram (ECG) signal, which can offer valuable information about myocardial perfusion and ventricular function [1]. However, the effectiveness of gated SPECT is at the expense of reduced photon count for each gate frame, which leads to increased noise in the reconstruction.

In recent years, there have been increasing interests in development of spatio-temporal reconstruction methods for reducing noise in gated SPECT. For example, an image summing method via optical flow over different gates was proposed in [2]; a Bayesian estimation approach was proposed in [3] based on a prior motion model; a Karhunen-Loeve transform method was used to de-correlate the gate images in [4]; a smoothing technique using polynomial fitting was described in [5]; in our previous work [6, 7], spatio-temporal reconstruction methods were developed to reduce the noise and motion blur based on motion compensation. These spatio-temporal methods aim to exploit the temporal correlation among the different gate

frames. Indeed, in cardiac SPECT the gate frames are essentially similar to each other except for the cardiac motion. In fact, they would be identical if it were not for the latter. Thus, it would be most effective to enforce smoothing along the motion trajectories in the gate frames. A challenge, however, is that the cardiac motion is not known *a priori*, and would have to be estimated from the noisy image data.

In this paper, we explore an alternative approach for spatio-temporal reconstruction of gated cardiac SPECT, which doesn't require specific motion knowledge. Rather than using an explicit temporal prior based on image motion, we model the time activities at each spatial location by a set of Fourier basis functions. This is motivated by the fact that, owing to the periodic nature of cardiac motion, the image intensity at each spatial location exhibits as a periodic function of the cardiac cycle. Thus, the periodic image motion can be modeled implicitly by periodic changes in image intensity in the resulting Fourier representation model. We first explored this idea recently in [8], where we demonstrated that a Fourier basis representation can be very effective for noise reduction while preserving cardiac motion. Encouraged by this initial success, in this work we further develop this approach by also including a spatial Gibbs prior. Consequently, not only a temporal constraint based on the periodicity of cardiac beating is used, but also a spatial smoothing constraint is enforced in the reconstruction.

In our proposed method, the different gate frames are estimated in a collective fashion by taking advantage of the statistics of the acquired data. Moreover, by varying the number of high order basis functions (i.e., high frequency components) used in the Fourier representation model, one can directly incorporate a temporal smoothing scheme into the reconstruction procedure in a spatially-adaptive fashion. Our evaluation results with gated Tc-99m labeled sestamibi imaging based on the NURBS-based cardiac-torso (NCAT) phantom demonstrate that the proposed approach can achieve significant noise reduction in reconstruction. The inclusion of spatial prior can further improve the accuracy of the reconstructed gate frames.

This work was supported by NIH/NHLBI Grant HL65425.

2. METHODS

2.1. Image model

In gated cardiac SPECT, the acquired projection data are binned into K gate intervals by using the ECG signal. The imaging model is described by the following

$$E[\mathbf{g}_k] = \mathbf{H}\mathbf{f}_k, k = 1, \dots, K \quad (1)$$

where \mathbf{g}_k , \mathbf{f}_k are vectors representing the acquired data (sinogram) and original image, respectively, in gate k , \mathbf{H} is the system matrix describing the imaging process in which each element h_{ij} represents the probability that a photon emitted at voxel j is detected at detector bin i , and $E[\cdot]$ is the expectation operator.

Our goal is to estimate the images \mathbf{f}_k given the sinogram data \mathbf{g}_k . Due to the low count level in the data and ill-conditioned nature of the system matrix \mathbf{H} , a direct inversion of the imaging equation in (1) to reconstruct individual gates would lead to very noisy images in gated SPECT. Instead, in this study we explore a joint reconstruction approach in which the different gate frames are reconstructed in a collective rather than individual fashion. The goal is to exploit the fact that the different gate frames are essentially similar to each other except for the cardiac motion.

2.2. Fourier basis representation model

Based on Fourier series expansion, we model the image activity at pixel j over different gates as

$$f_k(j) = \sum_{m=0}^{K-1} d_m(j) e_m(k), \quad j = 1, \dots, N, \quad k = 1, \dots, K \quad (2)$$

where $f_k(j)$ represents pixel j in gate k , $e_m(k)$ denotes the m -th Fourier harmonic basis function which has the form of $e_m(k) = \exp(\sqrt{-1} \cdot 2\pi m(k-1)/K) / \sqrt{K}$, $d_m(j)$ denotes its corresponding coefficient, and N denotes the number of pixels in a gate.

As can be seen, by varying the number of high order harmonics (i.e., high frequency components) included in the representation in (2), we can achieve different degrees of smoothing along the gate dimension. Thus, such a harmonic representation model offers the flexibility that one can directly incorporate a temporal smoothing scheme (i.e., across the gates) into the reconstruction procedure in a spatially-adaptive fashion. For example, the AC coefficients are known to be zero at background pixels which are not associated with the periodic cardiac motion, and thus are not necessary to be estimated. This can lead to fewer unknowns to estimate, and consequently, faster reconstruction algorithms. As demonstrated in our experiments, this can also lead to more accurate reconstruction results.

Substituting the image representation in (2) into the imaging model in (1), we obtain

$$E[\mathbf{g}_k] = \sum_{m=0}^{K-1} e_m(k) \mathbf{H} \mathbf{d}_m, \quad k = 1, \dots, K \quad (3)$$

where \mathbf{d}_m is a vector representing the collection of the m -th frequency coefficients $d_m(j)$ over all pixels.

Equation (3) relates the projection data directly to the frequency domain representation of the K gate frames. Our goal is to estimate the unknown coefficients \mathbf{d}_m associated with the different orders of harmonic basis functions.

2.3. Maximum a posteriori (MAP) estimate

For convenience, define $\mathbf{G} \triangleq [\mathbf{g}_1^T, \mathbf{g}_2^T, \dots, \mathbf{g}_K^T]^T$, which is a vector denoting the collection of acquired (sinogram) data in all K gates; similarly, $\mathbf{D} \triangleq [\mathbf{d}_1^T, \mathbf{d}_2^T, \dots, \mathbf{d}_K^T]^T$, denoting the collection of unknown coefficients of all K frequency components.

We seek a MAP estimate of the unknown coefficients, i.e.,

$$\hat{\mathbf{D}} = \arg \max_{\mathbf{D}} [\log p(\mathbf{G}; \mathbf{D}) + \log p(\mathbf{D})] \quad (4)$$

where $p(\mathbf{G}; \mathbf{D})$ is the likelihood function of \mathbf{G} parameterized by \mathbf{D} , and $p(\mathbf{D})$ is a prior distribution on \mathbf{D} .

In SPECT, the projection data are characterized by Poisson noise. The log-likelihood function has the following form

$$\log p(\mathbf{G}; \mathbf{D}) = \sum_{k=1}^K \sum_{i=1}^N \left[-\sum_{j=1}^N h_{ij} f_k(j) + g_k(i) \log \sum_{j=1}^N h_{ij} f_k(j) \right] \quad (5)$$

where $f_k(j)$ is parameterized by \mathbf{D} as in Eq. (2).

To further reduce the impact of Poisson noise, we introduce the prior term $p(\mathbf{D})$ in Eq. (4), which is used to impose a penalty when a pixel is significantly different in intensity from its spatial neighbors. Specifically, we use a Gibbs prior of the form

$$p(\mathbf{D}) \propto \exp\{-\beta_s U_s(\mathbf{D})\} \quad (6)$$

where $U_s(\mathbf{D})$ is an energy term defined as

$$U_s(\mathbf{D}) = \sum_{k=1}^K \sum_{j=1}^N \sum_{i \in \mathbb{N}_j} [f_k(j) - f_k(i)]^2 \quad (7)$$

where \mathbb{N}_j denotes a neighborhood region around pixel j . In our experiments, an 8-pixel neighborhood was used. In Eq. (6), β_s is a scalar weighting parameter used to control the degree of spatial smoothing.

Upon substituting the representation model in Eq. (2) into Eq. (7) and then applying the Parseval's identity, we can rewrite Eq. (7) as

$$U_s(\mathbf{D}) = \sum_{m=0}^{K-1} \sum_{j=1}^N \sum_{i \in \mathbb{N}_j} [d_m(j) - d_m(i)]^2 \quad (8)$$

From Eq. (8), we observe that the spatial variation of the image intensity in Eq. (7) is now represented equivalently by the spatial variation in the harmonic components.

2.4. Reconstruction algorithm

To find the MAP estimate in Eq. (4), we apply a generalized expectation-maximization (EM) algorithm [9]. For convenience, let vector \mathbf{S} denote the collection of auxiliary variables s_{ij}^k , which is defined as the number of photons emitted from within pixel j and detected in bin i in gate k .

Then, in the E-step the expected value of the complete-data log-likelihood function can be written as [10]

$$\begin{aligned} Q(\mathbf{D}, \hat{\mathbf{D}}) &= E \left[\log p(\mathbf{S}; \mathbf{D}) \mid \mathbf{G}, \hat{\mathbf{D}} \right] \\ &= \sum_{k=1}^K \sum_{i=1}^N \sum_{j=1}^N \left[p_{ij}^k \log \left(h_{ij} f_k(j) \right) - h_{ij} f_k(j) - E \left(s_{ij}^k \right) \right] \end{aligned} \quad (9)$$

where $\hat{\mathbf{D}}$ denotes the current estimate of \mathbf{D} , and the factors p_{ij}^k have the following form

$$p_{ij}^k = \left[h_{ij} \hat{f}_k(j) / \sum_{j'} h_{ij'} \hat{f}_k(j') \right] g_i^k \quad (10)$$

Note that in Eqs. (9) and (10) the quantity $f_k(j)$ is parameterized by \mathbf{D} via Eq. (2).

In the M-step, the estimate $\hat{\mathbf{D}}$ is updated as

$$\hat{\mathbf{D}}^{\text{new}} = \arg \max_{\mathbf{D}} \left\{ Q(\mathbf{D}, \hat{\mathbf{D}}^{\text{old}}) - \beta_s U_s(\mathbf{D}) \right\} \quad (11)$$

In our experiments, we used an iterative coordinate ascent algorithm [9,11], in which the unknown coefficients are updated for each pixel in turn. The Newton's method was applied for optimization of (11) at each step. For convenience, this method is referred to as DFT-MAP.

3. EVALUATION STUDY

3.1. Methods

In our evaluation study, the 4D NURBS-based cardiac-torso (NCAT) 2.0 phantom [12] was used to simulate gated SPECT imaging with Tc99m labeled sestamibi as the imaging agent. A perfusion defect with 25% intensity reduction was introduced in the anterior-lateral region of the left ventricle. The simulation was based on a Philips Prism 3000 SPECT system with a low-energy high-resolution (LEHR) collimator. The projections were 64×64 bins with a pixel size of 0.634 cm. For a circular camera rotation of 28.5 cm radius, 64 projection sets were collected for each gate frame for a total of 16 gates. The average spatial resolution at the location of heart in the reconstructed slices was approximately 1.3 cm full-width at half-maximum (FWHM). Poisson noise was introduced at a level of 4 million total counts for the whole acquired data as in a typical clinical acquisition. Neither scatter nor attenuation effects were considered in the simulation.

For preliminary evaluation of the spatio-temporal reconstruction approach, we used a transversal slice (#37) of the phantom. Figure 1 shows the first gate of this slice, along with a magnified view of the myocardium. The use of simulated images allowed us to quantitatively evaluate the reconstructed images where the ground truth was known.

To quantify reconstruction accuracy, we computed the signal to noise ratio (SNR) of the myocardium in the reconstructed images. The SNR of a reconstructed image $\hat{\mathbf{f}}$ is defined as

$$\text{SNR} = 10 \log_{10} \left[\frac{\|\mathbf{f}\|^2}{\|\mathbf{f} - \hat{\mathbf{f}}\|^2} \right] \quad (12)$$

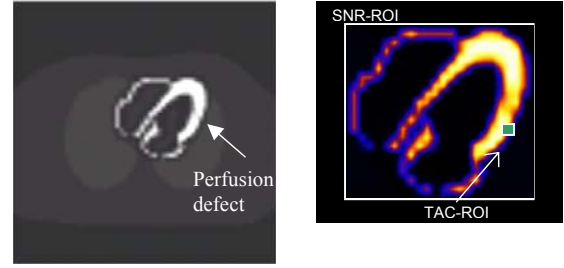


Fig. 1. Slice #37 of the NCAT phantom (left) and magnified view of ROIs in quantitative evaluation of results (right).

where \mathbf{f} denotes the known truth. In our experiments, the SNR was computed for the myocardium ROI (shown in Fig. 1) and averaged over the 16 gates.

Also, to demonstrate the effect of temporal smoothing on cardiac motion, we also computed the time-activity curve (TAC) of an ROI selected on the LV wall (shown in Fig. 1). As the wall moves in and out of this ROI during the beating cycle, its average intensity will vary accordingly, and thus, it serves as a good indicator on the degree of temporal smoothing caused by the different methods.

In our experiments, the AC coefficients were assumed zero and not reconstructed at pixels outside the myocardium region (indicated in Fig. 1).

For comparison purposes, we also considered a post-reconstruction temporal filtering approach for noise reduction, in which the 16 different gates were first reconstructed separately by using the classical ML-EM algorithm, then low-pass filtered along the gate dimension at each pixel location by truncating the higher-order frequency coefficients in the Fourier domain. This method is referred to as ML-LP in the following.

3.2. Results

In Fig. 2 we summarize the SNR results achieved by our proposed method DFT-MAP, the post-reconstruction filtering method ML-LP and the post-filter method from 20 noise realizations. The abscissa in Fig. 2 represents the highest order of harmonic components used in the reconstruction. Moreover, to demonstrate the effect of spatial smoothing, results are also given in Fig. 2 for different values of spatial smoothing parameter β_s . Note that when $\beta_s=0$ it corresponds to no spatial smoothing enforced. For each parametric setting, the number of iterations was determined based on the best SNR achieved.

From Fig. 2 we can see that the SNR of the myocardium region decreases monotonically with the order of harmonic functions used in the reconstruction. This demonstrates that the noise is increasingly associated with higher order harmonic components. In all cases, the DFT-MAP method is more accurate than ML-LP. This shows that it is more effective to incorporate temporal smoothing into reconstruction (as in the proposed method) than to apply post-reconstruction filtering.

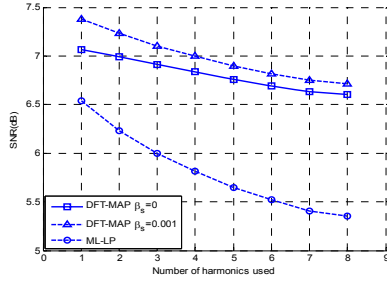


Fig. 2. SNR results obtained by DFT-MAP and ML-LP.

In Fig. 3 we show the reconstructed TAC of the TAC-ROI (indicated in Fig. 1) obtained from 20 different noise realizations by the DFT-MAP method with the number of harmonics set at one, three, and five, respectively. As can be seen, as the number of harmonics increased, the reconstructed TAC on average approaches closer to the ideal TAC (smaller bias), but the variance also increases (more noisy images). In addition, the introduced spatial prior can significantly reduce the variance. As reference, the ideal TAC curve was obtained from noiseless reconstruction of the phantom using the ML algorithm (40 iterations).

Finally, in Fig. 4 we show a set of typical reconstructed images by the DFT-MAP method with the order of harmonics fixed at three, where only the myocardium is shown for clarity; the ideal images are also shown for comparison. As can be seen, the LV wall is less noisy in the images with $\beta_s=0.001$ than that without spatial prior ($\beta_s=0$). Moreover, the wall shape in these reconstructed images follows closely that of the ideal, indicating that the harmonic representation at order three can faithfully model the wall motion for reconstruction.

4. CONCLUSIONS

We proposed a spatio-temporal approach for gated cardiac SPECT, in which Fourier basis functions were used to regulate the periodic temporal activities across the different gates. Our preliminary evaluation results demonstrate that this approach can yield much more accurate reconstruction of gated frames in cardiac SPECT. In future, we plan to further evaluate the proposed method using task-based performance metric (e.g. a channelized Hotelling observer for perfusion defect detection).

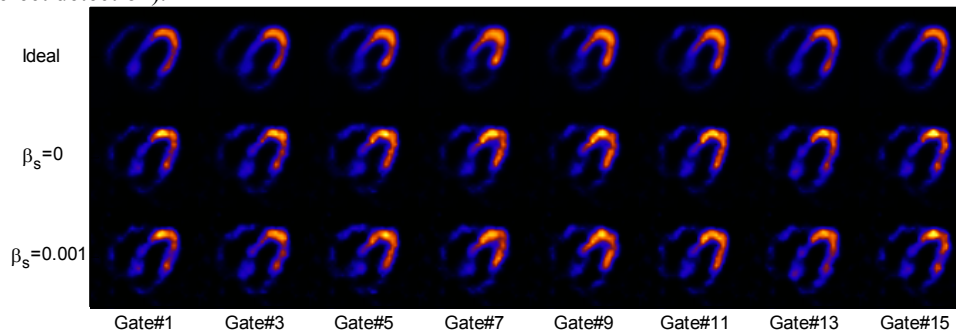


Fig. 4. Top row: noiseless EM reconstruction; Middle row: no spatial prior ($\beta_s=0$); Bottom row: spatial prior with $\beta_s=0.001$.

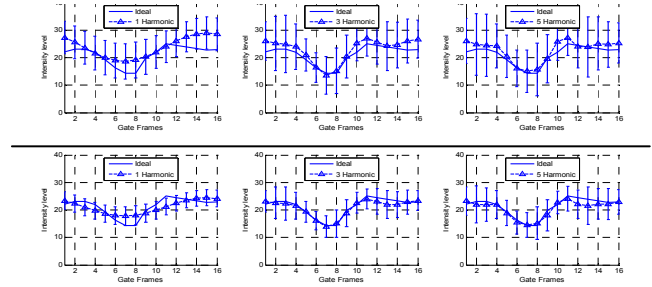


Fig. 3. TACs obtained from 20 noise realizations by DFT-MAP with different number of harmonics. Top row: no spatial prior $\beta_s=0$; Bottom row: spatial prior with $\beta_s=0.001$.

5. REFERENCES

- [1] E. G. Garcia, "Imaging guidelines for nuclear cardiology procedures I," *J. Nucl. Card.*, vol. 3, pp. G1-G46, 1996.
- [2] G. J. Klein, B. W. Reutter, and R. H. Huesman, "Non-rigid summing of gated PET via optical flow," *IEEE Trans. Nucl. Sci.*, vol. 44, 1997.
- [3] D. S. Lalush and B. M. W. Tsui, "Block-iterative techniques for fast 4D reconstruction using a prior motion models in gated cardiac SPECT," *Phys. Med. Biol.*, vol. 43, pp. 875-886, 1998.
- [4] M. V. Narayanan, M. A. King, *et al.*, "Application of the Karhunen-Loeve transformation to 4D reconstruction of cardiac gated SPECT images," *IEEE Trans. Nucl. Sci.*, vol. 46, pp. 1001-1008, 1999.
- [5] J. Peter, R.J. Jaszczak, B. F. Hutton and H. M. Hudson, "Fully Adaptive Temporal Regression Smoothing in Gated Cardiac SPECT Image Reconstruction," *IEEE Trans. Nucl. Sci.*, Vol. 48, No. 1, 2001.
- [6] J. G. Brankov, Y. Yang and M. N. Wernick, "Spatio-temporal processing of gated cardiac SPECT images using deformable mesh modeling," *Med. Phys.*, vol. 32, no. 9, pp. 2839-2849, 2005.
- [7] M. Jin, Y. Yang, *et al.*, "Four-dimensional reconstruction of gated cardiac SPECT with attenuation and scatter compensation," *Proc. Inter. Symposium Medical Imaging: Macro to Nano*, 2007.
- [8] X. Niu, M. Jin and Y. Yang, "Reconstruction of gated cardiac SPECT using DFT basis functions," *Proc. Asilomar Conference on Signals, Systems, and Computers*, Pacific Grove, CA, Nov. 4-7, 2007.
- [9] T. Herbert and R. Leahy, "A generalized EM algorithm for 3-D Bayesian reconstruction from Poisson data using Gibbs priors," *IEEE Trans. Med. Imag.*, vol. 8, pp. 194-202, 1989.
- [10] D. S. Lalush and M. N. Wernick. *Iterative Image Reconstruction*. In: M. N. Wernick and J. N. Aarsvold, editors. *Emission Tomography: the fundamental of PET and SPECT*, Elsevier Academic Press, 2004.
- [11] C. A. Bouman and K. Sauer, "A unified approach to statistical tomography using coordinatedescent optimization," *IEEE Trans. Imag. Proc.*, vol. 5, pp. 480-492, 1996.
- [12] W. P. Segars, *Development of a new dynamic NURBS-based cardiac-torso (NCAT) phantom*, Ph.D. thesis, The University of North Carolina, 2001.